

SCALING OF STIFFENED PANELS SUBJECTED TO IMPACT LOADING

Leonardo M. Mazzariol, Miguel A. G. Calle, Roberto E. Oshiro and Marcilio Alves

*Group of Solid Mechanics and Structural Impact, Department of Mechatronics and Mechanical
Systems Engineering, University of São Paulo, São Paulo 05508-900, Brazil,
<http://www.gmsie.usp.br>*

Keywords: Scaling, Ship Collision, Strain-rate sensitivity.

Abstract. The impact behaviour of a reinforced structure, similar to the ones found in ships, was studied both experimentally and numerically. The model was experimental and numerically tested while the prototype was investigated numerically only. The scaled impact mass was calculated according to a special formulation which takes into account the distortion of scaling laws due to the material strain-rate sensitivity. Experimental results were used to corroborate the theoretical model, also probed by a numerical simulation of the impact event.

1 INTRODUCTION

Ship collision events and ways to mitigate their consequences have been studied by many authors (ISSC, 2003; 2006). The inherent difficulties of real-scale experiments made numerical simulation an important tool to evaluate structural integrity of existent ships as well as different construction techniques in order to improve their safety. Despite powerful numerical simulation techniques it is always necessary experimental tests to corroborate a new design.

These experiments should be performed in models of reduced scale in face of the large size of a prototype. Laws that correlate the behaviour of a scaled model to a prototype are called for here. For example, Blok et al. (1983) developed experiments involving scaled model of lateral ship collision against a protected jetty focusing only on the analyses of the hydrodynamic water mass surrounding the ships. Tabri et al. (2008) developed experiments involving scaled model of a ship collision focusing on the ship hydrodynamics. The Froude scaling law of similarity was followed but it resulted in non scaling of some forces. The external shapes of the ship models were similar to the large-scale ships, but not the materials involved as the struck ship was made of solid steel and the striking ship made of polyurethane foam.

Given all the technical and economical difficulties to develop full-scale ship collision tests (Carlebur, 1995) some researches analyse the ship structure behaviour in a collision event by performing experimental tests on some ship structural parts. Hagbart and Amdahl (2009) analysed the structural response of a stiffened hull structure when penetrated by a steel indenter analogous to a ship stranding event. It was demonstrated that the resistance of the stiffened structure is increased while its ductility is decreased. The plate-stiffener intersection introduces stress concentration so controlling the global resistance of the structure. For this reason it is important to study not only the external mechanics but also the mechanics of ship structural members.

The aim of this paper is to compare classical similarity procedure with a different approach that takes the strain-rate sensitivity of a tested component into account. The chosen geometry is a stiffened plate made of mild steel. Experimental and numerical simulation were performed so to compare the validity of the adopted scaling procedure.

In Section 2 details of the similarity procedures are described. Material characterization tests over a wide range of strain-rates and parameters fitting are presented in section 3. Section 4 presents experimental tests setup, data acquisition and results. Numerical analyses of the experiments are presented in Section 5, with Section 6 discussing the main findings and concluding in Section 7.

2 SIMILARITY

The technique in which a structure scaled by a factor β (model) is used to reproduce the real size structure (prototype) is termed similarity or similitude. This method has been extensively studied (Baker et al., 1991; Skoglund, 1967) and widely applied in many works (Neuberger et al., 2007; Jones, 1995). For the impact phenomena, the scaling factors for the main variables are long known and summarized in Table 1. In order to achieve the perfect similarity, the Π theorem asserts that all predominant dimensionless numbers of the model must be equal to the corresponding prototype dimensionless numbers (Fox and McDonald, 1998)

$$(\Pi_i)_m = (\Pi_i)_p \tag{1}$$

where the subscripts m and p stand for model and prototype, respectively.

Nevertheless, it is also known that structures under dynamic loads usually do not follow scaling laws. It is due to effects such as material strain-rate sensitivity, material failure, material thermal response, gravity, etc. When a model cannot be related to the corresponding prototype by a single geometric scaling factor, it is assigned as imperfect similarity or a distorted model. Many works have reported this behaviour for scaled models (Drazetic et al., 1994; Gregory, 1995; Booth et al., 1983; Oshiro and Alves, 2004).

variable	factor	variable	factor
length, L	β	time, t	β
displacement, δ	β	velocity, V	1
mass, G	β^3	strain rate, $\dot{\epsilon}$	$1/\beta$
strain, ϵ	1	acceleration, A	$1/\beta$
stress, σ	1	force, F	β^2

Table 1: Factors relating model variables to the prototype

Recently, Oshiro and Alves (2009) proposed a method that takes the strain-rate effect into account. The initial impact velocity is changed so that the increase of yield stress due to strain-rate is compensated, according to

$$\beta_v = \beta^{q/(q-2)}, \tag{2}$$

where $\beta_v = V_m/V_p$ and q is the material constant of the Norton equation (Lemaitre and Chaboche, 1991) that defines the dynamic yielding stress, σ_d dependence to strain rate,

$$\sigma_d = \sigma_0 (\dot{\epsilon}/\dot{\epsilon}_0)^q. \tag{3}$$

Here, σ_0 is the quasi-static yielding stress, $\dot{\epsilon}_0$ the strain rate at σ_0 . In the present study, an adaptation of this method is made; instead of changing the impact velocity, the impact mass factor is altered in order to take the strain rate into account, i.e. $\beta_v = 1$ and $\beta_G \neq \beta^3$. First, the indirect similitude technique was employed (Drazetic et al., 1994). Instead of mass-length-time, the basis is comprised by initial velocity, V_0 , dynamic yielding stress, σ_d , and impact mass, G . The analysis of the main variables of the phenomena impact generates (Oshiro and Alves, 2004)

$$\Pi_1 = [A^3 G / (V_0^4 \sigma_d)], \tag{4}$$

$$\Pi_2 = [t^3 \sigma_d V_0 / G], \tag{5}$$

$$\Pi_3 = [\delta^3 \sigma_d / G V_0^2], \tag{6}$$

$$\Pi_4 = [\dot{\epsilon} G^{1/3} / (\sigma_d V_0)^{1/3}] \text{ and} \tag{7}$$

$$\Pi_5 = [\sigma / \sigma_d]. \tag{8}$$

The mass factor is obtained from equation (6),

$$(\Pi_3)_m = (\Pi_3)_p \rightarrow \frac{\beta^3 \beta_\sigma}{\beta_G \beta_V^2} = 1.$$

For the correction through the impact mass, $\beta_V = 1$, but $\beta_G \neq \beta^3$. As a result,

$$\beta_G = \beta^3 \beta_\sigma. \quad (9)$$

From equation (7),

$$(\Pi_4)_m = (\Pi_4)_p \rightarrow \beta_\varepsilon = (\beta_\sigma / \beta_G)^{1/3}. \quad (10)$$

Moreover, equation (3) generates

$$\beta_\sigma = \frac{(\sigma_d)_m}{(\sigma_d)_p} = \frac{\sigma_0 (\dot{\varepsilon}_m / \dot{\varepsilon}_0)^q}{\sigma_0 (\dot{\varepsilon}_p / \dot{\varepsilon}_0)^q} = \left(\frac{\dot{\varepsilon}_m}{\dot{\varepsilon}_p} \right)^q = (\beta_\varepsilon)^q, \quad (11)$$

and by inserting equation (11) into equation (10) one obtains

$$\beta_\sigma^{1/q} = \left(\frac{\beta_\sigma}{\beta_G} \right)^{1/3} \rightarrow \beta_G = \beta_\sigma^{(q-3)/q}. \quad (12)$$

Finally, the ratio between the model and prototype mass is generated by inserting equation (12) into equation (9)

$$\beta_G = \beta^3 \beta_\sigma^{q/(q-3)} \rightarrow \beta_G = \beta^{3-q}. \quad (13)$$

Equation (13) relies only on the scaling factor, β , and the material parameter, q . The structure material is rigid perfectly plastic and σ_d is given by equation (3). Being m the structure mass, equation (13) is valid for the condition $G \gg m$. This limitation arises from a characteristic of similarity technique: it does not distinguish variables with the same dimension. As a result, if the impact mass is changed, the method considers that the structure mass is modified by the same factor. In fact, it cannot be done in real experiments. In spite of that, even when the mass structure is not changed, equation (13) can be applied within small errors if $G \gg m$.

The factors for the other variables are obtained from equations (4) to (8)

$$\Pi_1 = \frac{A^3 G}{V_0^4 \sigma_d} \rightarrow \frac{\beta_A \beta_G}{\beta_\sigma} = 1 \rightarrow \beta_A = \beta_G^{1/(q-3)} \rightarrow \beta_A = \frac{1}{\beta}, \quad (14)$$

$$\Pi_2 = \frac{t^3 \sigma_d V_0}{G} \rightarrow \beta_t = \beta_G^{1/(3-q)} \rightarrow \beta_t = \beta, \quad (15)$$

$$\Pi_4 = \dot{\varepsilon} \left(\frac{G}{\sigma_d V_0} \right)^{1/3} \rightarrow \beta_\varepsilon \left(\frac{\beta_G}{\beta_\sigma} \right)^{1/3} = 1 \rightarrow \beta_\varepsilon = \beta_G^{1/(q-3)} \rightarrow \beta_\varepsilon = \frac{1}{\beta} \text{ and} \quad (16)$$

$$\Pi_5 = \frac{\sigma}{\sigma_d} \rightarrow \beta_\sigma = \frac{\beta_G}{\beta^3} \rightarrow \beta_\sigma = \frac{1}{\beta^q}. \quad (17)$$

Consequently, the factors used to transpose the model response to the prototype are given by equations (13) to (17). As can be noticed, they are different from the factors shown in Table 1. It is because Table 1 does not consider the yielding stress increase due to strain rate effect and the scaling factor, as can be seen in the fifth relationship in the first column, $\beta_\sigma = 1$.

3 MATERIAL CHARACTERIZATION TESTS

3.1 Low strain rate material properties

The material properties of the mild steel used to manufacture the components were obtained from standard tensile tests. The tensile specimens were cut from the main lamination direction of the 1 mm thickness plate and their dimensions are according to the ASTM sheet-type Rectangular Tension Test Specimen. A universal testing machine, Instron 3369 model, was employed for the tests under different frame velocities. The crosshead velocity of 0.2 mm/min was used as quasi-static reference curve. The other frame velocities employed were 1, 30, 150 and 300 mm/min which results in strain rates in the range of 0.0001 to 0.05 s⁻¹. See Figure 1.

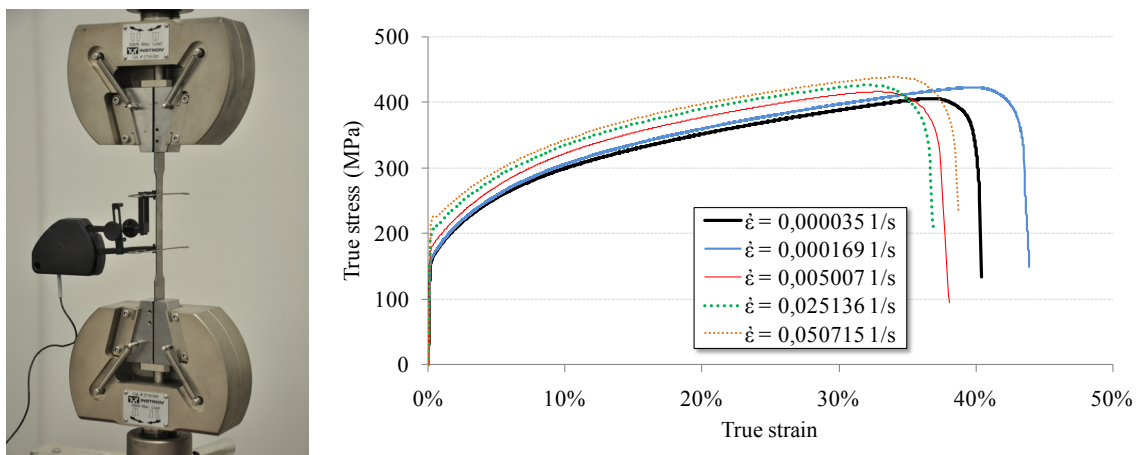
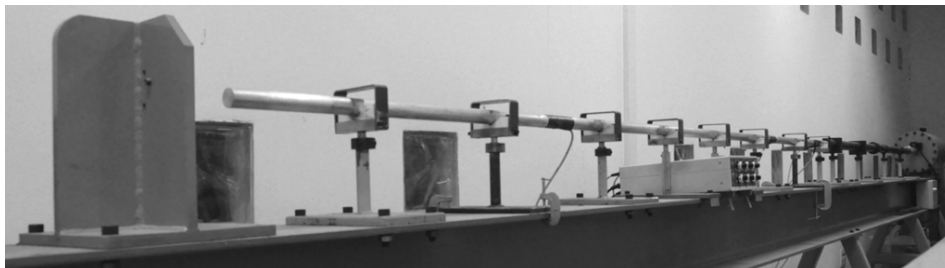


Figure 1: True strain-stress curves of mild steel obtained for low strain rates.

3.2 High strain rate material properties

The high strain rate properties of the mild steel were obtained from Split Hopkinson Pressure Bar tests. The 6 mm diameter disc specimens were cut also from the 1 mm thickness plate. The experiments were carried out for pressures of 0.8, 1.2 and 1.6 bar, resulting in strain-rates in the range from 3000 to 9000 s⁻¹. The resultant true strain stress curves are shown in Figure 2.



(a)

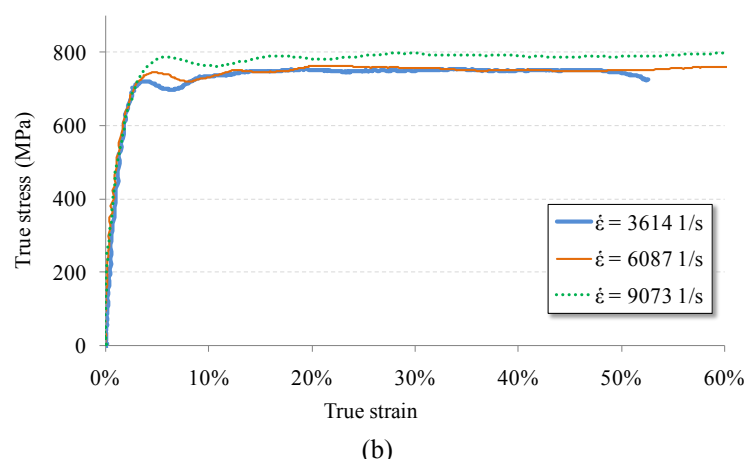


Figure 2: (a) Split Hopkinson Pressure Bar. (b) Representative true strain-stress curves of the mild steel obtained for each pressure.

3.3 Calibration of strain rate sensitivity parameters

The Norton parameters of the mild steel were obtained from the experimental data, including the low and high strain rates results considering a total strain of 20%. In Figure 3 it can be seen two groups of points which represent the two natures of the tests. The resultant Norton parameters were calculated as $q = 0.049$ and $\dot{\epsilon}_0 = 0.0009$. Table 2 summarises the material parameters.

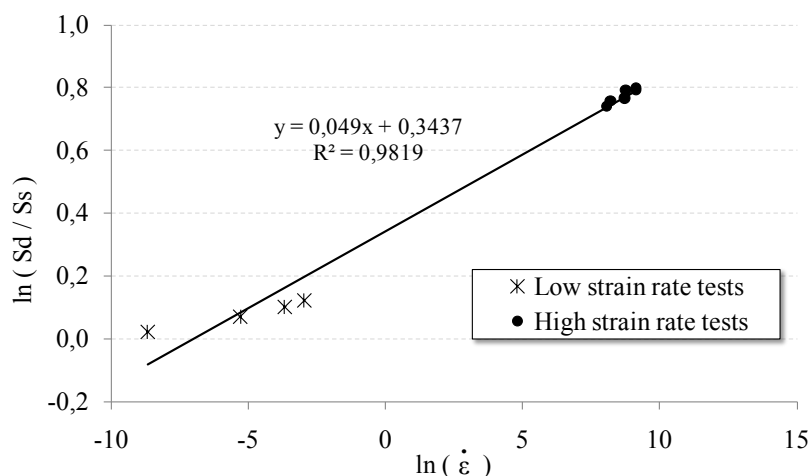


Figure 3: Calculated Norton parameters.

Young modulus	Poisson coefficient	Density	Yield stress	Hardening	Norton-Hoff parameter q	$\dot{\epsilon}_0$
[GPa]	[-]	[kg/m ³]	[MPa]	[MPa]	[-]	[1/s]
200	0.3	7850	154	402	0.049	9×10^{-4}

Table 2: Mild steel mechanical properties.

4 EXPERIMENTS

Experiments involving marine structures may be complex to carry out in real scale, not only due to cost issues, but also because it is important to control most test parameters. On the present study, both the dimensions of the real-scale structure and the difficulty to precisely control a heavy indenter positioning led to a reduced scale approach. As a result, the dimensions of the model were scaled 20 times smaller than the prototype. The calculation of mass correction is presented on item 4.1.

In order to represent a ship component the chosen structure (Figure 4a) was clamped on both ends and struck at mid span by a mass. Steel parts (blocks) were bolted to a box to reach the specified mass value. The striker was made with 1045 steel; defined by a combination of a cylinder of 50mm diameter, with a conical lower part with apex angle of 50°, fitted in a 12.5mm radius sphere nose (see Figure 5b). This assembly is attached between two linear guides.

The stiffened panel was painted in white with black dots in random pattern to aid visualization. That panel was bolted to a support and then to the anvil (Figure 5b).

Indenter velocity was recorded by a laser doppler vibrometer made by Polytec with controller model OFV-3020 and laser model OFV-323, sampled at 500kHz. The laser device was put under the anvil, and the light beam passed through 12mm diameter holes until it reached a special reflexive 3M tape that improves the quality of the reflected light. Tests were also recorded with a Photron APX-RS High Speed Camera at 4500fps using a 50mm lens.

4.1 Calculation of mass correction

The geometry of prototype is a T-shaped panel made of 20mm-thick mild steel. Main plate is 1 m wide by 4 m in length, with 0.4 m height reinforcement welded on both sides on the central line. Impact load is provided by a 120 tons indenter at 3 m/s. The dimensions of scaled models are obtained by reducing the prototype by a factor $\beta=1/20$, resulting in stiffened panel with 1mm thickness, 50mm wide, 200mm in length, with 20mm height. These geometries were cut with laser in the lamination direction and welded with laser (Figure 4a and Figure 4b).

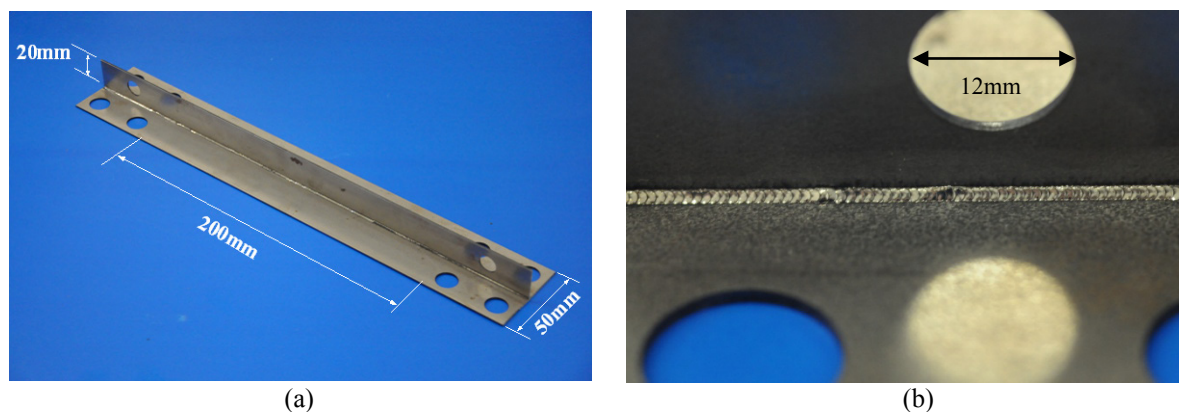


Figure 4: Stiffened panel model dimensions (a). Laser weld details (b).

Mass is associated to scaled dimensions according to a cubic rule, i.e., a reduction of β in all dimensions gives a β^3 reduction in mass. From 120 ton in prototype's indenter, 15kg or $\beta_G = 1,25 \times 10^{-4}$ is obtained for classic scaled model's indenter, or MLT-Model (MLT stands

for mass-length-time similarity approach). Furthermore, inserting β factor and $q = 0.049$ (Norton parameter) obtained in Section 3, in equation (13), VSG-model's (initial Velocity-Dynamic Yield Stress – Impact Mass similarity approach) mass factor $\beta_G = 1,45 \times 10^{-4}$ is obtained. Table 3 summarizes the scaling factors and test conditions.

Geometry	Scaling factor β [-]	Impact Mass [kg]	Mass Factor β_G [-]	Velocity [m/s]
Prototype	1	120×10^3	1	3,0
MLT-Model	1/20	15.0	1.25×10^{-4}	3,0
VSG-Model	1/20	17.4	1.45×10^{-4}	3,0

Table 3: Load and initial conditions applied in experiments

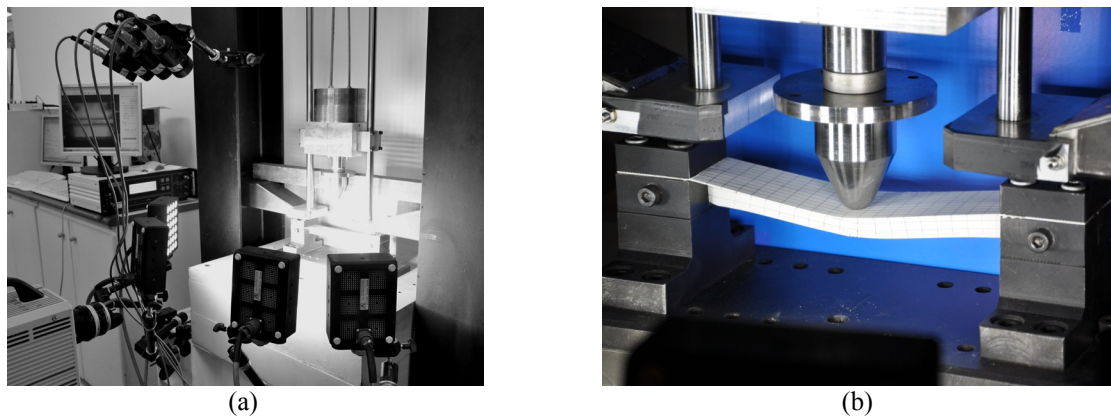
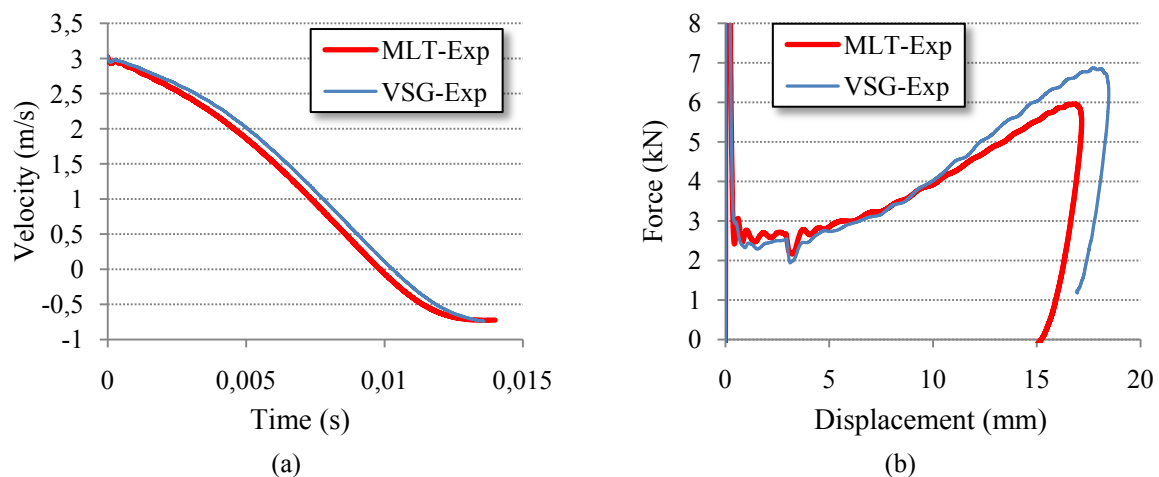


Figure 5: (a) Illumination, Camera and test apparatus. (b) Component and support after test

4.2 Experimental results

The obtained velocity signal was filtered using moving average and then differentiated to obtain the acceleration and then, force. Integrating, displacement was obtained. Plots on Figure 6a shows the treated velocity signal for both experiments and Figure 6b and c, the calculated variables force and displacement. The abrupt change on velocity in the initial instant of impact causes the force to rise to 20kN on both specimens.



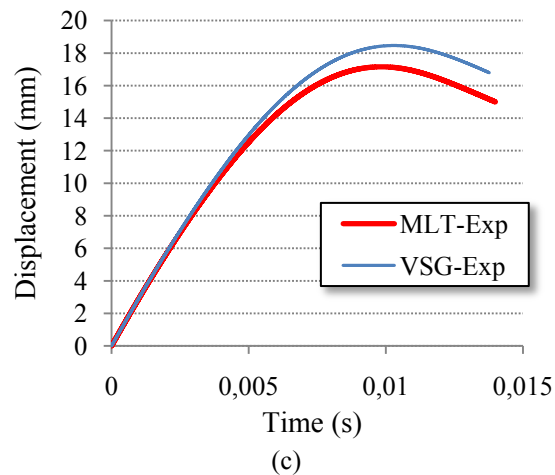


Figure 6: Velocity (a), force (b) and displacement results of experiments

5 SIMULATIONS

Numerical model was created using Altair Hypermesh 9.0 and LS-dyna 971 R4.2.1 Revision 53450 was used as explicit dynamics numerical solver.

The stiffened panel was modelled using shell elements with squares of 0.5mm to properly reproduce the folds. Both main plate and stiffener were modelled as one-point-integrated Belytschko-Tsay shell elements with five integration points through thickness. That formulation was preferred due to a better computational efficiency if compared to Hughes-Liu shell (Lsdyna, 2007a). Material model used for panel was bilinear elasto-plastic with strain-rate sensitivity curve according to Norton equation, with the properties listed in Table 2. In addition, viscoplastic formulation for rate effects was also defined (Lsdyna, 2007b). The assembly of indenter was simplified removing masses, box and linear guides, reducing numerical geometry to indenter and flange, as shown in Figure 7a. Then those were modelled as rigid body with density calculated to match de impact mass. Contact between indenter and panel was defined with friction of 0.1 and stiffness penalty factor equal to 10.0. Also, critical time step scale factor was set to 0.3.

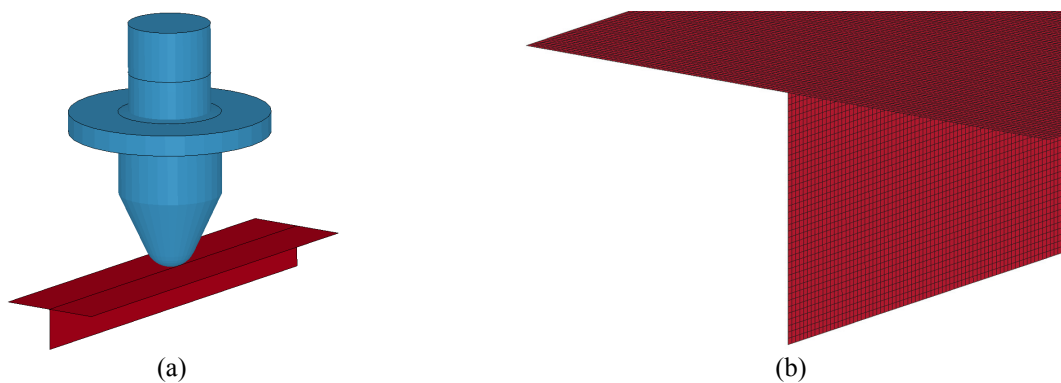


Figure 7: (a) Components. (b) Detailed mesh for stiffened panel

The panel support was simplified applying constraints directly on 'T' sections boundaries in all degrees of freedom (Figure 7a). Indenter was allowed to move only towards the panel. Both experiments were slightly displaced (2 mm) from stiffener projection line, what was also considered in simulation set-up. Velocity in simulation was obtained from as rigid body information.

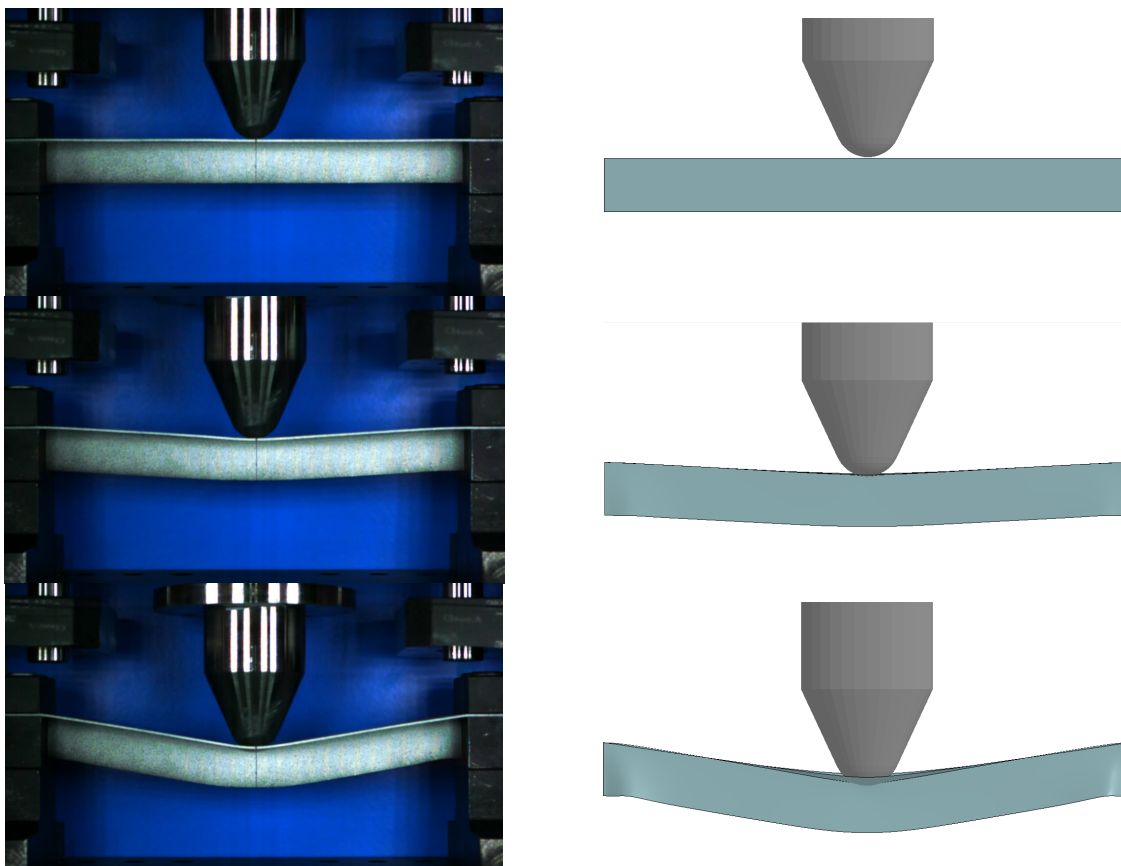


Figure 8: Experiment and simulation comparison for MLT model. Images at 0.0s, 0.002s and 0.0095s.

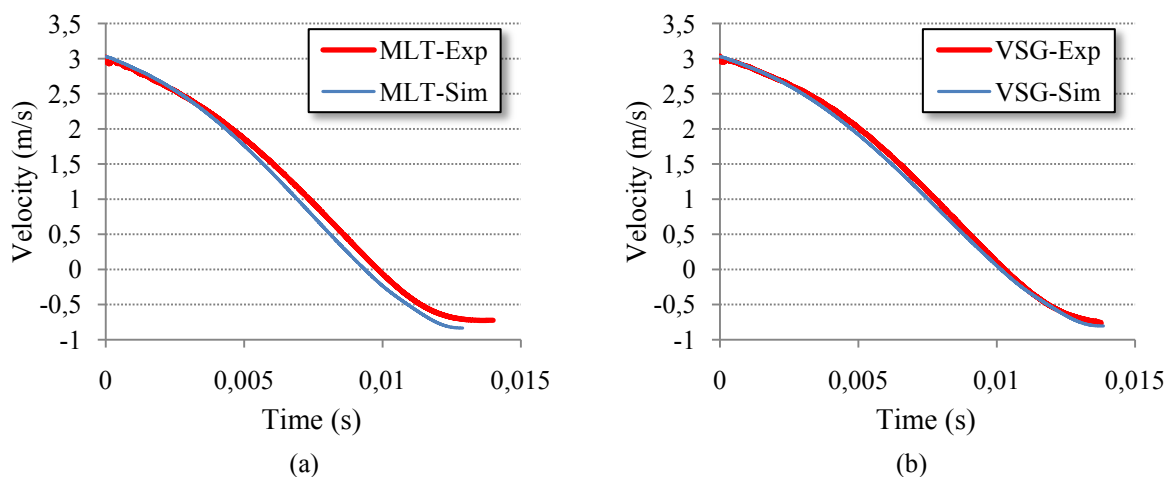


Figure 9: Simulation and experiments results for MLT (a) and VSG (b) scaled models.

Simulation and experiment velocity results are plotted in Figure 9a and Figure 9b. In a similar procedure used for data treatment in experimental curves, force (acceleration) and displacement were obtained and are plotted in Figure 10a,b and Figure 10c,d, respectively. As can be seen, plots show a reasonable correlation between simulation and experiments,

however VSG simulation curves are closer to the experiments than MLT curves.

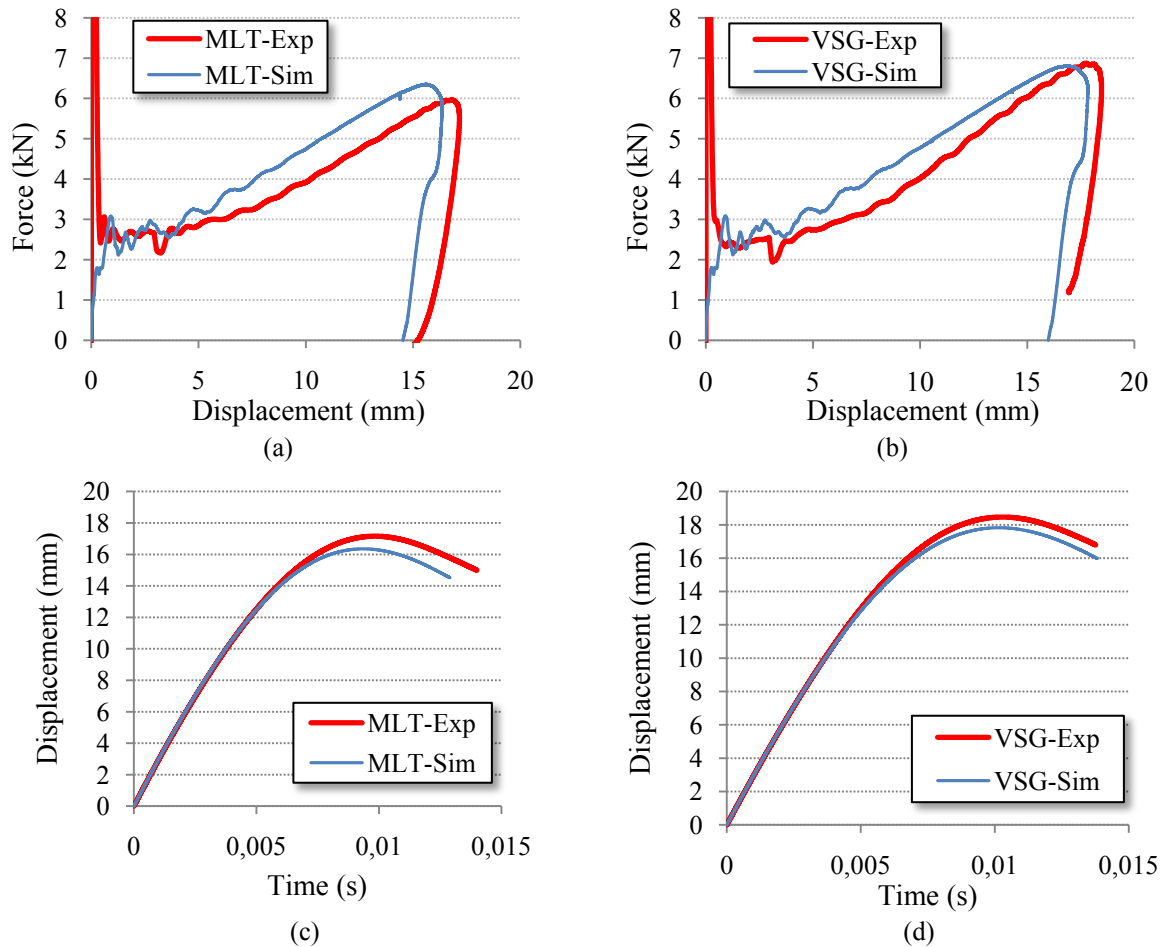


Figure 10: Simulation and experiment comparison on forces and displacement for MLT(a, c) and VSG (b,d)

In order to be compared to the prototype, scaled model results must be multiplied by a factor depending on the similarity approach used. Thus, time, displacement and force from MLT-model were multiplied by factors from Table 1. For the VSG-model, time and displacement follow the same rule, however force requires a different factor $\beta_F = \beta^{2-q}$, which is obtained from eq. (13) and (14). Scaled forces were plotted in Figure 11 and displacement in Figure 12.

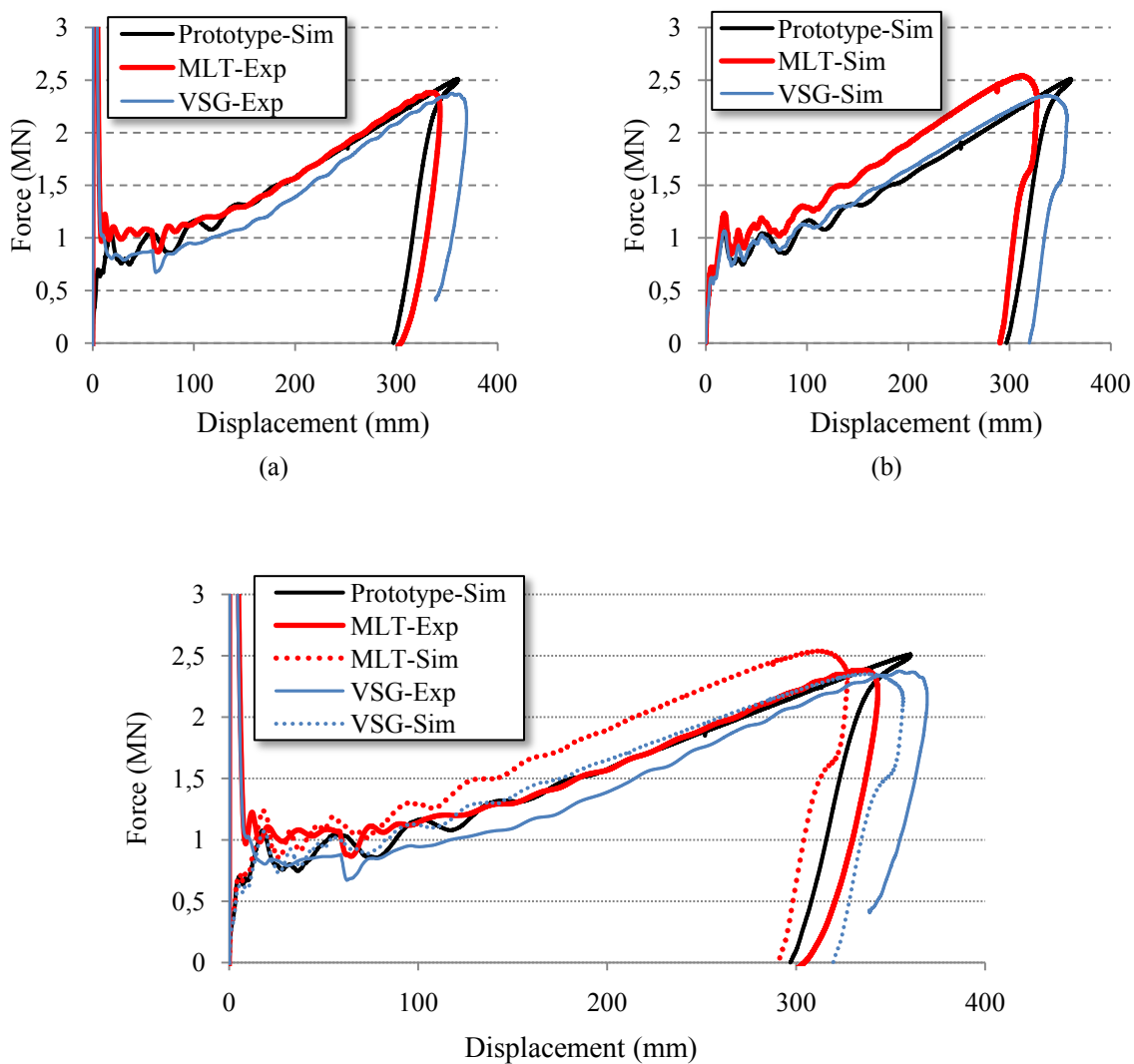
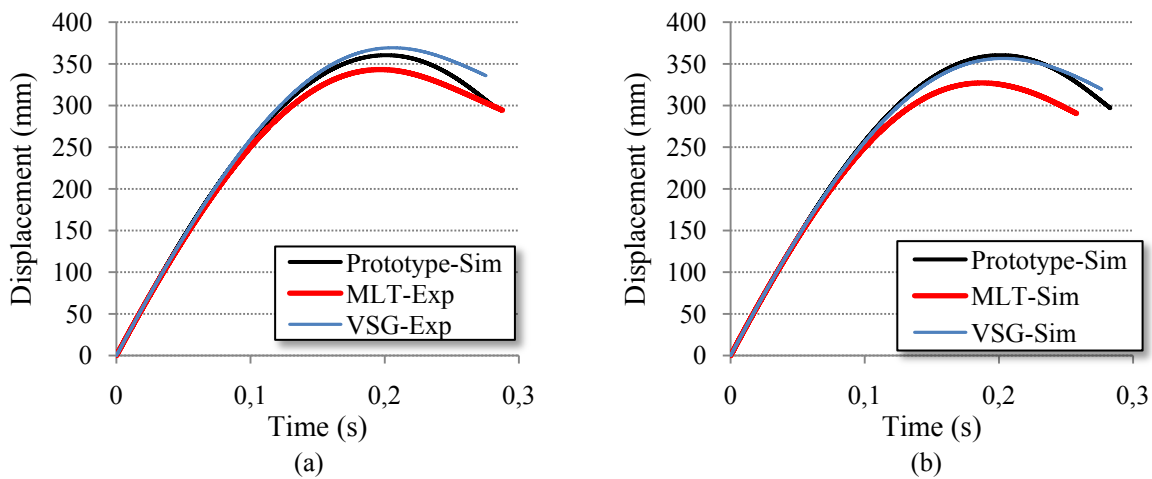


Figure 11: Experiment (a) and Simulation (b) force results scaled in reference to prototype simulation



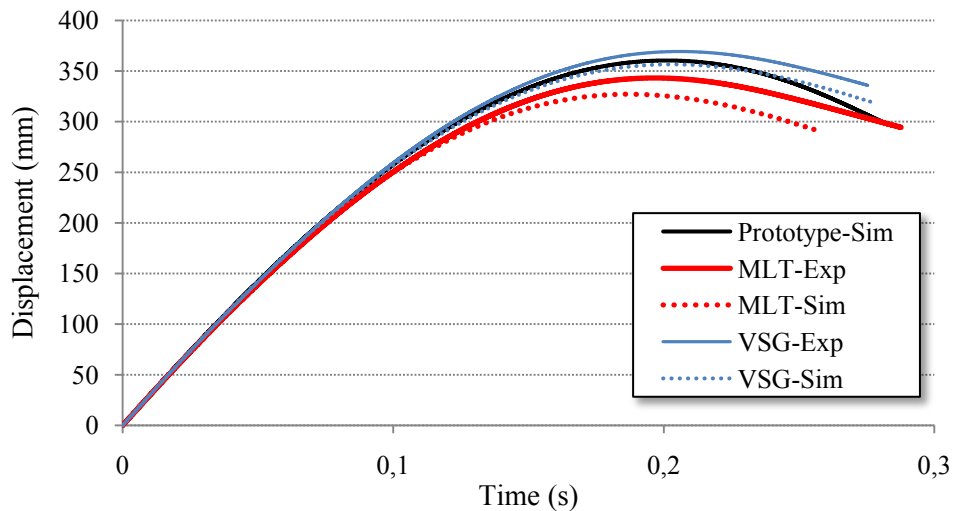


Figure 12: Experiment (a) and Simulation (b) displacement results scaled in reference to prototype simulation.

6 DISCUSSIONS

The applied similarity method was intended to scale structures modelled as rigid perfectly plastic. However, experimental material tests showed that a bilinear model represents better the real material behaviour. Although this mild steel does not match the required conditions for the applied similarity procedure, the method was employed to the model since the plastic deformations are predominant in the phenomena.

The differences of the maximum displacement between simulations and corresponding experimental tests are of 4,9% and 3,58% for MLT-model and VSG-model, respectively. As for the forces at maximum displacement, the difference is of 6,5% and 1,0%, respectively. Part of that discrepancy in scaled models can be attributed to an overestimation of support stiffness in numerical analysis, since it was implemented as campled edges. Nevertheless, in the slow motion video it was observed that the support bent towards centre and slips for the MLT model. Also, that stiffer behaviour (Figure 10a and b) may be attributed, in part, for simple material numerical modeling.

Although results of VSG and MLT models are similar, the VSG curves are closer to the real size structure simulation. This can be observed mainly in simulation results (Figure 11b), where scaled forces of VSG simulation model at 300 mm of displacement reduces discrepancy from 12,44% of MLT simulation model to 1,8%. This can also be noticed in displacement curves (Figure 12), where the difference is reduced from 9,2% to 0,8%.

As discussed in section 2, the correction method that changes the impact mass requires the condition $G \gg m$. In the present work, the mass striker is 17.4kg and the structure mass is 0.170kg, i.e., $m/G = 0.0098$. Therefore, the structure inertia is negligible while compared to the striker one.

7 CONCLUSIONS

This paper presented a different approach for scaling of structures subjected to impact load. Via experiments and simulations of scaled models in addition to similarity laws, it was shown that the behaviour of a real-scale structure can be predicted. And, for this method, no further information of structure response was needed to calculate the correction of impacted mass,

whilst it depends only on the Norton material parameter q and scale factor β .

Even though the presented method corrects only plastic portion and does not evaluate plastic hardening, reasonable results could be achieved for the present case. Further improvement on material model will aid experiment to simulation correlation.

ACKNOWLEDGEMENTS

The authors would like to thank the Brazilian research funding FINEP for the financial support. The authors are also grateful to Rafael Traldi Moura and Caio César Brasilino Fukumori for their assistance.

REFERENCES

- Alsos, H.S. On the resistance to penetration of stiffened plates, Part I - Experiments. *International Journal of Impact Engineering*, 36: 799-807, 2009.
- Baker, W.E., Westine, P.S., Dodge, F.T. *Similarity methods in engineering dynamics: Theory and practice of scale modeling*. Amsterdam: Elsevier Science Publishers, 1991. 348 p.
- Blok, J.J.; Brozius, L.H.; Dekker, J.N. The Impact Loads of Ships Colliding With Fixed Structures. In: *Proceedings of the Offshore Technology Conference*, OTC 4469, Dallas-TX-United States, 1983.
- Booth, E.; Collier, D.; Miles, J. Impact scalability of plated steel structures. In: Jones, N.; Wierzbicki, T. (Ed). *Structural Crashworthiness*. London: Butterworths, 1983, p. 136-174.
- Carlebur, A.F.C. Full-scale collision tests. *Safety Science*, 19: 171-178, 1995.
- Drazetic, P. et al. Applying non-direct similitude technique to the dynamic bending collapse of rectangular section tubes. *International Journal of Impact Engineering*, v. 15: 797-814, 1994.
- Gregory, L.F. Replica model scaling for high strain-rate events. *International Journal of Impact Engineering*, 16: 571-583, 1995.
- ISSC. *Comittee V.3: Collision and Grounding*. 15th International Ship and Offshore Structures Congress (ISSC), San Diego, USA, 2003.
- ISSC. *Comittee V.1: Collision and Grounding*. 16th International Ship and Offshore Structures Congress (ISSC), Southampton, UK, 2006.
- Jones, N. Some comments on the scaling of inelastic structures loaded dynamically. In: Batra, R.C.; Mal, A.K.; Macsithigh, G.P. (Ed.). *Impact, Waves and Fracture*, AMD-Vol.205, ASME (1995), p. 153-167.
- Lemaitre, J.; Chaboche, J.L. *Mechanics of solids materials*. Cambridge: Cambridge University Press, 1991. 584 p.
- Lsdyna. *LS-DYNA Theory manual*. Version 971. Livermore Software Technology Corporation; 2007a.
- Lsdyna. *LS-DYNA Keyword Reference Manual*. Version 971. Livermore Software Technology Corporation; 2007b.
- Neuberger, A.; Peles, S.; Rittel, D. Scaling the response of circular plates subjected to large and close-range spherical explosions. Part I: Air-blast loading. *International Journal of Impact Engineering*, 34: 859-873, 2007.
- Oshiro, R.E.; Alves, M. Scaling impacted structures. *Archive of Applied Mechanics*, 74: 130-145, 2004.
- Oshiro, R. E.; Alves, M. Scaling of structures subject to impact loads when using a power law constitutive equation. *International Journal of Solids and Structures*, 46: 3412-3421, 2009.

- Skoglund, V.J. *Similitude: Theory and Applications*. Pennsylvania: International Textbook Company, 1967.
- Tabri, K.; Määttänen, J.; Ranta, J. Model-scale experiments of symmetric ship collisions. *Journal of Marine Science and Technology*, 13: 71-84, 2008.